RSC Advances

ROYAL SOCIETY OF CHEMISTRY

www.rsc.org/advances

Cite this: DOI: 10.1039/c0xx00000x

www.rsc.org/xxxxxx

ARTICLE TYPE

Synthesis of bright upconversion submicrocrystals for high-contrast imaging of latent-fingerprints with cyanoacrylate fuming

Han-Han Xie[a,b], Qian Wen[a], Hao Huang[a,c], Tian-Ying Sun[a], Penghui Li[b], Yong Li [b], Xue-Feng Yu[b], Qu-Quan Wang*[a]*

Received (in XXX, XXX) Xth XXXXXXXXX 20XX, Accepted Xth XXXXXXXXX 20XX
DOI: 10.1039/b000000x

Upconversion particles (UCPs) as a new generation of imaging agent are gaining prominence due to their unique optical properties. Herein, we report the synthesis of bright UCPs for high-contrast imaging of latent-fingerprints with cyanoacrylates-fuming (CA-fuming). The hexagonal-phase and rod-shaped $NaYF_4$:Yb,Er/Ce submicrocrystals (0.5 × 1.0 μm in dimension) coated with polyethylenimine (PEI) are synthesized using a dopant-controlled strategy and exhibit extremely stronger UC fluorescence than their nanosized analogues. The appropriate particle size and good surface properties of the UCPs make them easily come into the holes formed on fibrous layers of fingerprint ridges after fumed by CA. Compared with downconversion fluorescent materials, the UCPs exhibit the ability to suppress background fluorescence interference for obtaining high-contrast fingerprint images under near-infrared (NIR) light irradiation. Our results indicate that this strategy can successfully been applied to detect latent-fingerprints on various surfaces including non-porous and porous surfaces, and the fingerprints from different people can be identified. All of these benefits ensure this strategy an important tool in fingerprint detection and will find wide-ranging applications in forensic investigations and medical diagnostics.

Introduction

Fingerprints, which provide unique information about an individual, have been found wide applications in forensic investigations and medical diagnostics.[1,2,3] In most cases, the fingerprints are invisible to the naked eyes, referred as latent-fingerprints,[4] which require physical or chemical treatments to enable visualization. The earliest fingerprint detection techniques include ninhydrin solution[4] and iodine/benzoflavone spray.[5] Subsequently, a large number of research groups have developed techniques based on various spectroscopies, for example, mass spectrometry,[6] vibrational spectroscopy (infrared[7] and Raman[8]), and electro chemical microscopy.[9] In recent years, cyanoacrylate (CA)-fuming technique has been developed and widely applied in latent-fingerprint detection.[10,11]

Among these techniques, CA-fuming has been regarded as an extremely simple and most efficient method for latent-fingerprint detection on non-porous and porous surfaces.[10,11] Although the chemical process is still under debate,[12,13] the anionic polymerization of CA takes place, which is probably initiated by a variety of compounds contained in the residue constituting the fingerprint, such as amino acids, fatty acids and proteins. Thus, fingerprints can be efficiently detected as sticky white materials that form along the papillary ridges. However, the main limitation of CA-fuming technique arises from the white color taken from the detected fingerprints, which often lacks contrast with the light colored substrates.[14,15]

Fingerprint detection with fluorescence has recently been well-established and regarded as an efficient post-treatment for CA-fuming. Such post-treatments consist in staining the CA-fumed fingerprints with fluorescent dye solution or dusting the fingerprint with fluorescent powders.[16] The commonly used fluorescent materials include organic dyes (such as Ardrox,[17] Rhodamine 6G[18]), and semiconductor quantum dots (QDs, such as CdS,[19] CdSe[20]). These materials generally provide visible fluorescence under a shorter-wavelength ultraviolet (UV) light irradiation. Despite their advantages in enhancing the sensitivity, such conventional fluorescent materials often suffer from poor contrast due to the background luminescence while many actual substrates contain fluorophores.[21] Furthermore, due to the potential carcinogenesis of these materials, appropriate protection for laboratory workers and adequate waste elimination are required, which are expensive and require space.

Among currently developed fluorescent materials, upconversion particles (UCPs), particularly lanthanide-doped rare-earth crystals, are believed to be the focus of the next generation of imaging.[22-33] Different from conventional downconversion fluorescent materials, the UCPs can emit shorter-wavelength light under near-infrared (NIR) light excitation by converting two or more photons into a higher-energy output photon.[34,35] Since fluorophores in various substrates cannot be excited by NIR light, the imaging of latent-fingerprints with UCPs suffers less background fluorescence interference than conventional downconversion fluorescent material, thus can offer better optical contrast and higher detection sensitivity. Very recently, Quan Yuan et al. have established a fingerprint detection method by conjugating nanosized UCPs with lysozyme-binding aptamer, demonstrating

the applicability of UC fluorescence to suppress the substrate background fluorescence.[36] Furthermore, the rare-earth elements are generally harmless and the rare-earth UCPs can be directly synthesized in water which exhibit good biocompatibility *in vivo* applications.[37]

In this paper, we provide an easily performed strategy for high-contrast imaging of latent-fingerprints by the combination of bright UCPs with CA-fuming. The hexagonal-phase and rod-shaped $NaYF_4$:Yb,Er/Ce submicrocrystals (0.5 × 1.0 μm in dimension) coated with polyethylenimine (PEI) were synthesized using an established dopant-controlled strategy,[38] and exhibit much stronger UC fluorescence than their nanosized analogues. Compared with conventional downconversion fluorescent materials, the synthesized UCPs can efficiently suppress the background fluorescence interference for obtaining high-contrast fingerprint images. The bright UC fluorescence, suitable particle size and kind surface chemistry render them an ideal staining reagent for latent-fingerprint imaging with CA-fuming.

Experimental Section

Materials

Branched polyethylenimine (PEI, Mw=10000), ethanol, NaCl, NaOH, $RECl_3•6H_2O$ (RE=Y, Yb, Er, Ce) and NH_4F were purchased from Sigma-Aldrich. Rose Bengal (RB) (95%) was obtained from Aldrich (America). CdTe quantum dots (QDs) were purchased from Janus New-Materials Co., Ltd (Nanjing, China). CA was obtained from Deli group Co., Ltd (Shanghai, China). All the reagents were used as received without further purification.

Synthesis of PEI-coated $NaYF_4$:Yb,Er/Ce Submicrocrystals

In a typical procedure, growth solution was prepared by dissolving $RECl_3$ (RE: Y, Yb, Er and Ce) and NaCl in water with total RE and Na^+ ion concentrations of 0.5 mol/L. PEI stock solution (5 wt%) and NH_4F stock solution (1 mol/L) were prepared by dissolving them in water respectively. Then 1 mL of NaCl, 0.67 mL of YCl_3, 0.2 mL of $YbCl_3$, 0.03 mL of $ErCl_3$ and 0.10 ml of $CeCl_3$ were added to the mixture of 15 mL of ethanol and 5 mL of PEI. After 5 min vigorous agitation, an appropriate amount of NH_4F (F/Na ratio of 6) were added to the above solution and stirred for another 20 min. The mixture was then transferred to a Teflon-lined autoclave and heated at 200 ^oC for at least 3 h. By changing the reaction time and dopant concentration, the crystallite size of the products could be regulated. After cooling down to the room temperature, the resulting $NaYF_4$:Yb,Er/Ce were washed with ethanol and water three times and vacuum-dried at 70 ^oC for 2 h

Collection of Fingerprints

Volunteers were asked to wipe their fingertips across their foreheads or facial areas and then deposited their fingerprints on the surfaces which were cleaned with water and dried at room temperature before use. Surfaces investigated in this work include: compact disc, aluminium foil, glass slide, photocopy paper and hard paper. Banknotes were also under consideration since they were known to be a difficult semi-porous surface for fingerprints detection.

Fingerprint Detection by Combining UCPs with CA-fuming

CA-fuming was performed by a simple method. 1 mL NaOH with the concentration of 1 mol/L was dropped by the drip pipe to the pledget which was attached to the bottom of petri dish. Subsequently the equivalent volume of CA was added to the corresponding position. That was similar to a simple "Fuming box". Then the "Fuming box" was upside down on the prepared surfaces deposited the fingerprints. After 10 min fuming, the fingerprints on the various surfaces were processed with UCP powders by using squirrel brushes. Developed fingerprints were illuminated with a portable NIR laser at a wavelength of 980 nm (for UC imaging). Images were recorded by using the digital single-lens reflex camera equipped with a macro lens.

Instruments

The scanning electron microscopy (SEM) measurements were performed with a Siron FEI microscope. The transmission electron microscopy (TEM) measurements were performed with a JEOL 2010 HT microscope (operated at 200 kV). The X-ray powder diffraction (XRD) analysis was carried out on a Bruker D8 ADVANCE X-ray diffractometer with Cu Kα1 irradiation (λ=1.5406 Å). The Fourier transform infrared (FTIR) spectra were acquired through an Avatar-360 spectrometer. The UC emission spectra were obtained via a 980 nm continuous-wave (CW) diode laser and recorded by a spectrometer (Spectrapro 2500i Acton) with a liquid nitrogen cooled CCD (SPEC-10:100B, Princeton). The fluorescence images of fingerprints were recorded by a digital single-lens reflex camera (Canon, 650D, Japan) equipped with a macro lens. A ZF-5 portable UV lamp with 365 nm light radiation was used as excitation source in detection of fingerprints with RB and QDs.

Results and Discussion

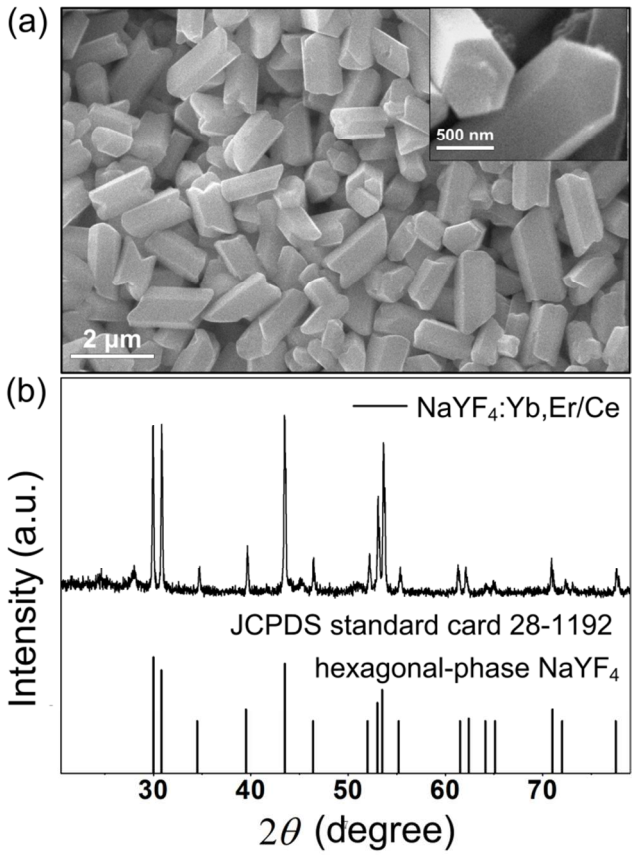

Figure 1: (a) SEM image and (b) XRD spectra of $NaYF_4$:Yb,Er/Ce submicrocrystals. Inset in (a) shows the regular hexagonal cross-section of the particles. The line spectrum in (b) corresponds to the literature data for hexagonal-phase $NaYF_4$ crystal (JCPDS standard card 28-1192).

The $NaYF_4$:Yb,Er/Ce submicrocrystals are synthesized using the established dopant-controlled strategy.[38] As shown in Figure 1a, the $NaYF_4$:Yb,Er/Ce submicrocrystals are rod-like with an average dimension of 0.5 × 1.0 μm. The inset image shows the regular hexagonal cross-section of the particles. Figure 1b illustrates XRD patterns of the $NaYF_4$:Yb,Er/Ce submicrocrystals. All the peaks are well indexed to the literature data of hexagonal-phase $NaYF_4$ crystal (JCPDS standard card 28-1192), which is generally considered as the most efficient host material for UC fluorescence.[39]

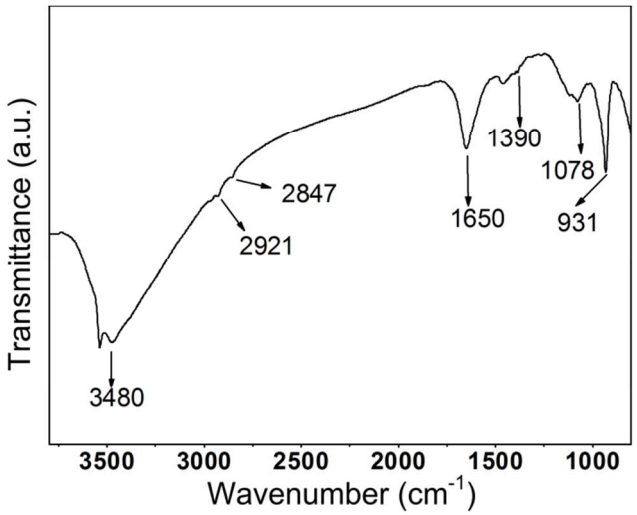

Figure 2: FTIR spectrum of $NaYF_4$:Yb,Er/Ce submicrocrystals.

The surface chemistry of the $NaYF_4$:Yb,Er/Ce submicrocrystals is investigated by FTIR. The PEI which has multiple amino groups on each polymer chain plays a vital role in the formation of the particles with favorable surface properties.[40,41] As shown in Figure 2, two strong bands at around 3480 and 1650 cm^{-1} in the FTIR spectrum correspond to OH stretching vibrations of surface hydroxyl groups, rendering the UCPs soluble and well dispersed in water. The presence of PEI on the particle surface is demonstrated by the existence of the characteristic absorption bands from internal vibration of amide bonds (around 1382 cm^{-1}) and CH_2 stretching vibrations (2863 and 2927 cm^{-1}) in the spectrum.[38,42] Furthermore, the absorption peaks at around 1078 and 931 cm^{-1} are assigned to C–C–O asymmetric stretching and symmetric stretching, respectively.[43] The hydrophilic and positively charged amino groups of PEI not only stabilize the UCPs in the solution but also can be used for covalently bonding to biomolecules.[40] Additionally, since PEI has low toxicity, it has been widely used *in vivo* bioapplications.[44]

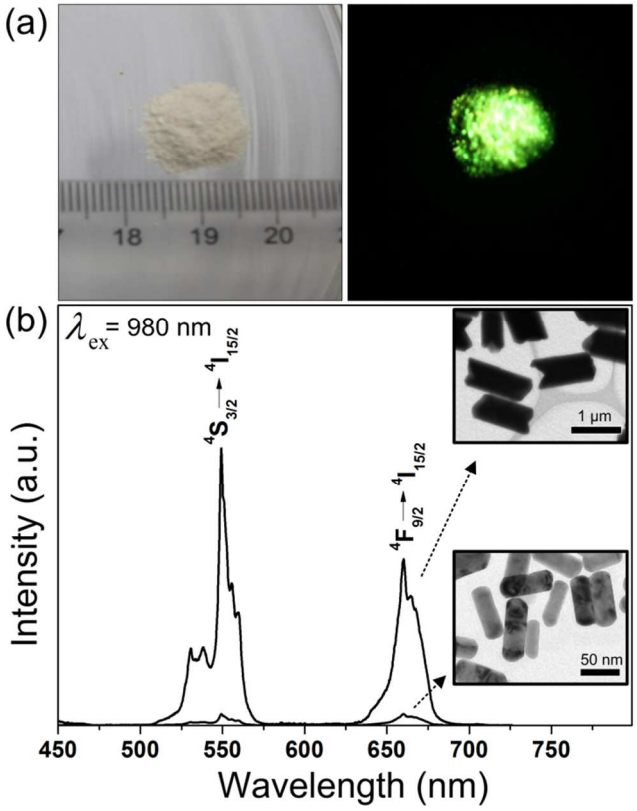

Figure 3: (a) Photographs of $NaYF_4$:Yb,Er/Ce powders under white light (left) and 980 nm laser illumination (right). (b) UC emission spectra and inset TEM images of submicron (up) and nanosized (down) $NaYF_4$:Yb,Er/Ce particles.

The UC fluorescence properties of the $NaYF_4$:Yb,Er/Ce submicrocrystals are further investigated. As shown in Figure 3a, bright green fluorescence can be observed from the $NaYF_4$:Yb,Er/Ce powders under a 980 nm laser illumination. Figure 3b displays the UC emission spectrum of the $NaYF_4$:Yb,Er/Ce submicrocrystals compared with their nanosized analogues synthesized using the same strategy just with different concentration of F^- ions. When excited with the 980 nm laser, the $NaYF_4$:Yb,Er/Ce submicrocrystals present two characteristic emission bands, which can be attributed to the 4f–4f transitions of Er^{3+} ions. The green emission originating from the $^2H_{11/2}$, $^4S_{3/2}\rightarrow{}^4I_{15/2}$ transition is observed at ~550 nm, whereas the red emission at ~660 nm is assigned to the $^4F_{9/2}\rightarrow{}^4I_{15/2}$ transition.[45] Furthermore, the $NaYF_4$:Yb,Er/Ce submicrocrystals exhibit more than twenty times stronger UC fluorescence than their nanosized analogues. The bright UC fluorescence and suitable particle size make them an ideal choice for high-contrast imaging of latent-fingerprints.

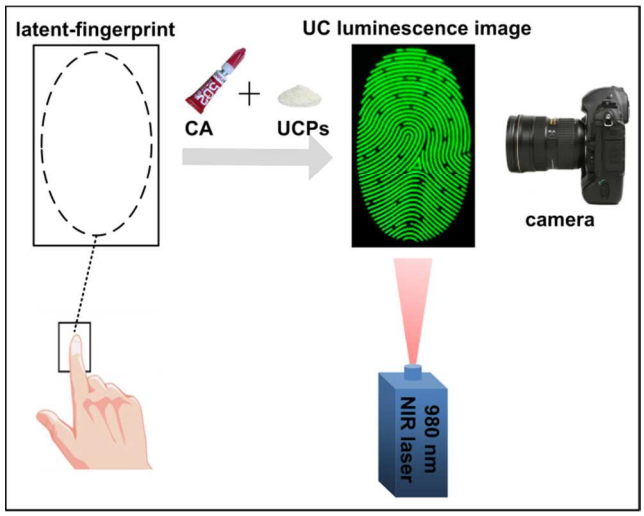

Figure 4: Strategy for latent-fingerprint detection with CA-fuming and UCPs.

The strategy of latent-fingerprint detection by using the $NaYF_4$:Yb,Er/Ce UCPs and CA-fuming is illustrated in Figure 4. In brief, after the fingerprint fumed by CA, the fingerprint is painted with the UCPs powders by using a squirrel brush. Then, the developed fingerprint is excited by a 980 nm NIR laser, and the image of fingerprint can be captured by a digital camera. Obviously, the developed strategy is convenient and easy to conduct without any complicated or expensive instrumentation.

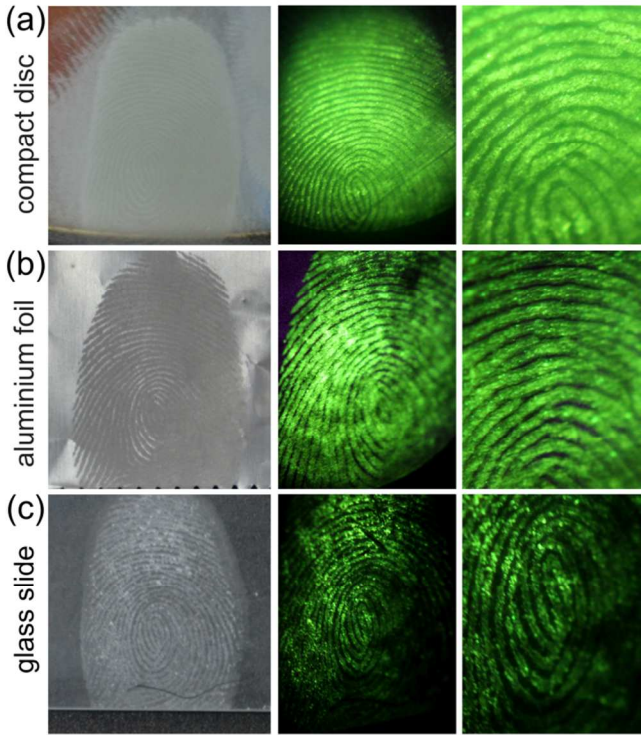

Figure 5: Photographs and UC luminescence images of CA-fumed fingerprints developed on a (a) compact disc, (b) aluminium foil, and (c) glass slide. Left: photographs of fingerprints; middle: luminescence images; right: magnified luminescence images. The fingerprints stained with UCPs were excited by a 980 nm NIR light.

The performance of the combination of bright UCPs with CA-fuming is tested on the smooth surfaces including compact disc, aluminium foil, and glass slide, all of which are daily used. As shown in Figure 5, the fingerprints on the smooth surfaces can be observed after the CA-fuming. When the UCPs are used, these fingerprints exhibit clear and bright luminescence under illumination with a 980 nm NIR light. The specific details of the fingerprint pattern, such as whorl and termination points can even be easily recognized at the magnified images. These results indicate that the UCPs exhibit a good affinity for fingerprints ridges to highlight the fingerprints with CA-fuming.

The mechanism of this strategy for fingerprint detection is analyzed. When a fingerprint was deposited on the surface, 99% of the moisture would quickly evaporate while few materials were left. The remaining materials generally included sodium chloride, potassium chloride and other inorganic materials (about 50%), as well as amino acids, fatty acids, proteins and other organic components. CA-fuming is known as an important method in fingerprint detection.[46,47] As a colorless and monomeric liquid, when CA was exposed to the air, probably initiated by the catalysis of water and alkali, the liquid formed vapour that would react with amino acids, fatty acids and proteins contained in the residue constituting the fingerprint. Consequently, a hard and white polymer known as polycyanoacrylate formed a fibrous layer on the fingerprint ridges, which contained many holes with diameters of around 1 to 2 micrometres.[48] In our strategy, the submicron UCPs with size of 0.5 × 1.0 μm were smaller than the holes in the fibrous layer, which made them easily came into the holes. The suitable size of the UCPs rendered them an ideal candidate in the staining of CA-fumed fingerprint.

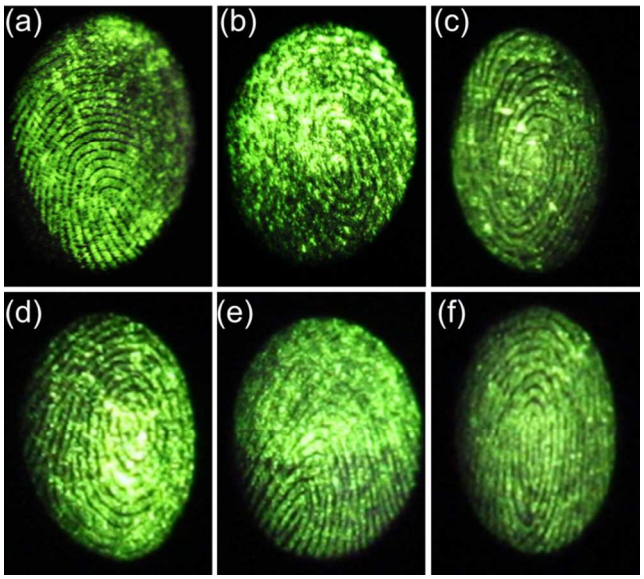

Figure 6: Luminescence images of fingerprints from six volunteers which were treated with CA-fuming and UCPs.

The applicability of this strategy for the detection of fingerprints from different people is further investigated. Figure 6 shows luminescence images of fingerprints from six volunteers under a 980 nm NIR light irradiation. It can be observed that the UC images display evident details of the fingerprint pattern, which will provide useful evidence for individual identification. These observations indicate that this strategy can be successfully applied to identify fingerprints from different people which demonstrate the good versatility of this method. Considering this advantage, it has the potential to be a convenient and efficient tool in criminal investigation.

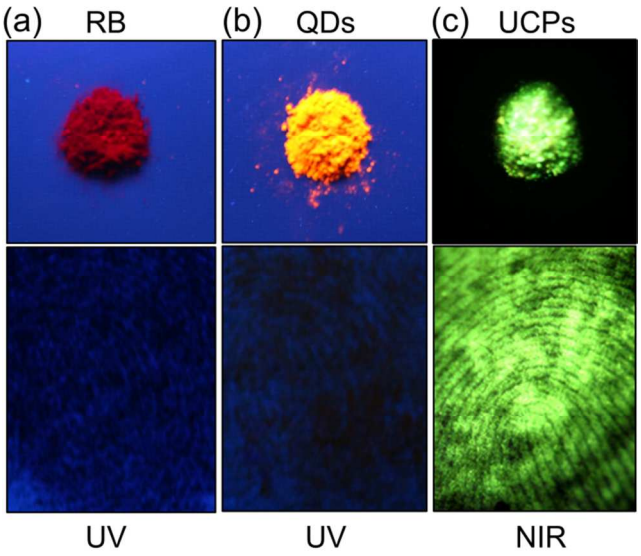

Figure 7: UC luminescence images of fingerprints (down) treated with (a) RB, (b) QDs, and (c) UCPs and the corresponding powders (up). RB and QDs were excited by a 365 nm UV light, while UCPs were excited by a 980 nm NIR light.

The benefit of the UCPs for fingerprint detection is further determined by using RB and CdTe QDs as control samples (Figure 7). All the fingerprints developed on photocopy papers are treated with CA-fuming before applied with the fluorescent powders. Fluorescence can be observed from the powders of both the RB and QDs under a 365 nm UV light radiation. However, the latent-fingerprints treated with them are hardly identified due to the strong interference from the background fluorescence of photocopy papers themselves, which greatly affect the imaging sensitivity. In contrast, the latent-fingerprints treated with the UCPs show bright fluorescence under a 980 NIR light irradiation, and a high-contrast luminescence image without any interference from background fluorescence is obtained. The results demonstrate that the strategy with UCPs can efficiently suppress the background fluorescence interference of substrates for obtaining high-contrast fingerprint image.

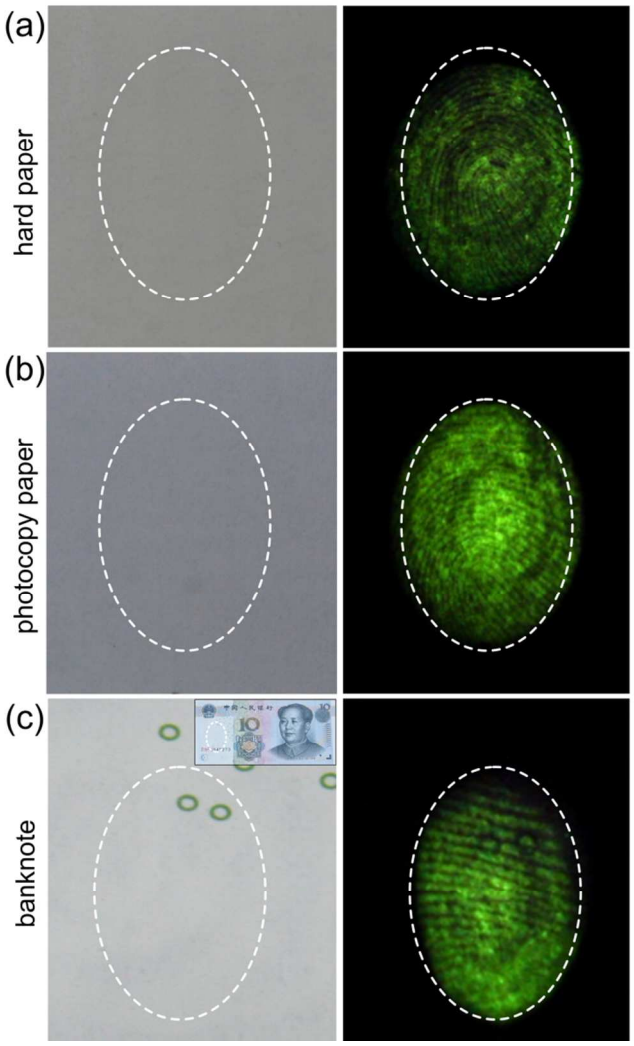

Figure 8: Photographs and luminescence images of CA-fumed latent-fingerprints developed on a (a) hard paper, (b) photocopy paper, and (c) banknote. Left: photographs of fingerprints in the white circle; right: luminescence images with a 980 nm NIR light.

It is known that the latent-fingerprints on light-colored surfaces are very difficult to be observed and photographed. Here, the applicability of the strategy for imaging of latent-fingerprints on three kinds of light-colored surfaces is investigated. Figure 8a shows a latent-fingerprint on a hard paper (with waterproof membrane on the surface), which is a typical non-porous surface. After the treatment with the CA-fuming and UCPs staining, a clear luminescence image of the latent-fingerprint can be obtained under a 980 nm NIR light irradiation. Compared with non-porous surfaces, fingerprints on porous surfaces such as photocopy papers are more difficult to be detected. Even so, clear UC luminescence image of the fingerprint on a photocopy paper can also be obtained with our strategy (Figure 8b). Beyond that, banknotes are considered as a semi-porous surface due to the intaglio printing and each of the denominations exhibits broadband luminescence. By using our strategy, clear luminescence image of fingerprint developed on a banknote can be observed and photographed, which exhibits the very good applicability of the developed strategy. As we all know, many crimes are related with the banknotes which will leave the fingerprints of the criminal. Therefore, the successful detection of the latent-fingerprints on banknotes will provide great help for crime detection.

Conclusions

In summary, an easily performed strategy has been established for high-contrast imaging of latent-fingerprints by the combination of bright UCPs and CA-fuming. The suitable particle size and kind surface properties of the UCPs make them suitable to combine with CA-fuming. Compared with downconversion fluorescent materials such as RB and QDs, the UCPs can efficiently suppress the background fluorescence interference for obtaining high-contrast fingerprint images under the 980 nm NIR light irradiation. Our results demonstrate that this strategy can be successfully applied to detect fingerprints on various surfaces including non-porous and porous surfaces and can be used to identify fingerprints from different people. Considering the strategy is convenient and easy to implement without any complicated or expensive instrumentation, it is believed that it will find widely applications in forensic investigations and medical diagnostics.

Acknowledgements

The authors acknowledge financial support from the National Program on Key Science Research of China (2011CB922201), the Natural Science Foundation of China (51372175), the Program of Public Interest Research and Capability Construction of Guangdong Province (2014A010105034), and the Technology & Innovation Commission of Shenzhen Municipality (JCYJ20130401160028777).

Notes and references

[a]*Department of Physics, Key Laboratory of Artificial Micro- and Nano-structures of Ministry of Education and School of Physics and Technology, Wuhan University, Wuhan, 430072, China.*
E-mail: qqwang@whu.edu.cn
[b]*Institute of Biomedicine and Biotechnology, Shenzhen Institutes of Advanced Technology, Chinese Academy of Sciences, Shenzhen, 518055, China.*
E-mail: xf.yu@siat.ac.cn
[c]*Shenzhen Research Institute, Wuhan University, Shenzhen, 518057, China*.

1 P. Hazarika, D. A. Russell, *Angew. Chem. Int. Ed.,* 2012, **51**, 3524.
2 K. Li, W. W. Qin, F. Li, X. C. Zhao, B. W. Jiang, K. Wang, S. H. Deng, C. H. Fan, D. Li, *Angew. Chem.,* 2013, **125**, 11756.
3 E. Stauffer, A. Becue, K. V. Singh, K. R. Thampi, C. Champod, P. Margot, *Forensic Sci. Int.,* 2007, **168**, e5.
4 S. Odén, H. B. Von, *Nature,* 1954, **173**, 449.
5 K. Flynn, P. Maynard, E. D. Pasquier, C. Lennard, M. Stoilovic, C. Roux, *J. Forensic Sci*., 2004, **49**, 707.
6 D. R. Ifa, N. E. Manicke, A. L. Dill, R. G. Cooks, *Science,* 2008, **321**, 805.
7 D. T. Burns, J. K. Brown, A. Dinsmore, K. K. Harvey, *Anal. Chim. Acta.,* 1998, **362**, 171.
8 W. Song, Z. Mao, X. J. Liu, Y. Lu, Z. S. Li, B. Zhao, L. H. Lu, *Nanoscale,* 2012, **4**, 2333.
9 X. N. Shan, U. Patel, S. P. Wang, R. Iglesias, N. J. Tao, *Science,* 2010, **327**, 1363.
10 D. M. Keating, J. J. Miller, J. Forensic Sci., 1993, 38, 197.

11 L. A. Lewis, R. W. Smithwick, G. L. Devault, B. Bolinger, S. A. Lewis, J. Forensic Sci., 2001, 46, 214.
12 P. Czekanski, M. Fasola, J. Allison, *J. Forensic Sci.* 2006, **51**, 1323.
13 S. P. Wargacki, L. A. Lewis, M. D. Dadmun, *J. Forensic Sci.,* 2007, **52**, 1057.
14 B. K. Chesher, J. M. Stone, W. F. Rowe, *Forensic Sci. Int.,* 1992, **57**, 163.
15 H. J. Kobus, R. N. Warrener, M. Stoilovic, *Forensic Sci. Int.,* 1983, **23**, 233.
16 L. Liu, Z. L. Zhang, L. M. Zhang, Y. C. Zhai, *Forensic Sci. Int.,* 2009, **183**, 45.
17 M. M. McCarthy, *J. Forensic Ident.,* 1990, **40**, 75.
18 W. D. Mazzella, C. J. Lennard, *J. Forensic Ident.,* 1995, **45**, 5.
19 E. R. Menzel, M. Takatsu, R. H. Murdock, K. Bouldin, K. H. Cheng, *J. Forensic Sci.,* 2000, **45**, 770.
20 M. Sametband, I. Shweky, U. Banin, D. Mandler, J. Almog, *Chem. Commun.,* 2007, 1142.
21 R. L. Ma, E. Bullock, P. Maynard, B. Reedy, R. Shimmon, C. Lennard, C. Roux, A. McDonagh, *Forensic Sci. Int.,* 2011, **207**, 145.
22 T. Y. Cao, Y. Yang, Y. Gao, J. Zhou, Z. Q. Li, F. Y. Li, *Biomaterials,* 2011, **32**, 2959.
23 G. S. Yi, G. M. Chow, *Adv. Funct. Mater.,* 2006, **16**, 2324.
24 F. Wang, R. R. Deng, J. Wang, Q. X. Wang, Y. Han, H. M. Zhu, X. Y. Chen, X. Y. Liu, *Nat. Mater.,* 2011, **10**, 968.
25 F. Wang, Y. Han, C. S. Lim, Y. H. Lu, J. Wang, J. Xu, H. Y. Chen, C. Zhang, M. H. Hong, X. G. Liu, *Nature,* 2010, **463**, 1061.
26 S. J. Liu, L. L. Zhang, T. S. Yang, H. R. Yang, K. Y. Zhang, X. Zhao, W. Lv, Q. Yu, X. L. Zhang, Q. Zhao, X. M. Liu, W. Huang, *ACS Appl. Mater. Interfaces,* 2014, **6**, 11013.
27 L. Zhou, B. Z. He, J. C. Huang, Z. H. Cheng, X. Xu, C. Wei, *ACS Appl. Mater. Interfaces,* 2014, **6**, 7719.
28 G. S. Yi, H. C. Lu, S. Y. Zhao, G. Yue, W. J. Yang, D. P. Chen, L. H. Guo, *Nano Lett.,* 2004, **4**, 2191.
29 D. K. Chatterjee, A. J. Rufaihah, Y. Zhang, *Biomaterials,* 2008, **29**, 937.
30 M. Nyk, R. Kumar, T. Y. Ohulchanskyy, E. J. Bergey, P. N. Prasad, *Nano Lett.,* 2008, **8**, 3834.
31 L. Y. Wang, Y. D. Li, *Chem. Mater.,* 2007, **19**, 727.
32 L. Josephson, M. F. Kircher, U. Mahmood, Y. Tang, R. Weissleder, *Bioconjugate Chem.* 2002, **13**, 554.
33 H. Zhang, Y. J. Li, I. A. Ivanov, Y. Q. Qu, Y. Huang, X. F. Duan, *Angew. Chem. Int . Ed.,* 2010, **49**, 2865.
34 S. F. Chen, B. Peng, F. Lu, Y. Mei, F. Cheng, L. L. Deng, Q. H. Xiong, L. H. Wang, X. W. Sun, W. Huang. *Adv. Optical Mater.,* 2014, **2**, 442.
35 W. Wang, W. J. Huang, Y. R. Ni, C. H. Lu, Z. Z. Xu, *ACS Appl. Mater. Interfaces,* 2014, **6**, 340.
36 J. Wang, T. Wei, X. Y. Li, B. H. Zhang, J. X. Wang, C. Huang, Q. Yuan, *Angew. Chem.,* 2014, **126**, 1642.
37 X. F. Yu, Z. B. Sun, M. Li, Y. Xiang, Q. Q. Wang, F. F. Tang, Y. L. Wu, Z. J. Cao, W. X. Li, *Biomaterials,* 2010, **31**, 8724.
38 X. F. Yu, M. Li, M. Y. Xie, L. D. Chen, Y. Li, Q. Q. Wang, *Nano Res.,* 2010, **3**, 51.
39 F. Wang, X. Liu, *Chem. Soc. Rev.,* 2009, **38**, 976.
40 F. Wang, D. K. Chatterjee, Z. Li, Y. Zhang, X. Fan, C. Wang, *Nanotechnology,* 2006, **17**, 5786.
41 W. T. Godbey, K. K. Wu, A. G. Mikos, *J. Controlled Release,* 1999, **60**, 149.
42 T. Y. Sun, D. Q. Zhang, X. F. Yu, Y. Xiang, M. Luo, J. H. Wang, G. L. Tan, Q. Q. Wang, P. K. Chu, *Nanoscale,* 2013, **5**, 1629.
43 J. Kurdi, A. Kumar, *Polymer*, 2005, **46**, 6910.
44 A. Baker, M. Saltik, H. Lehrmann, I. Killisch, V. Mautner, G. Lamm, G. Christofori, M. Cotten, *Gene Ther.,* 1997, **4**, 773.
45 S. Heer, K. Kömpe, H. U. Güdel, M. Haase, *Adv. Mater.,* 2004, **16**, 2102.
46 L. Karlinszky, G. Harkai, *Forensic Sci. Int.,* 1990, **46**, 29.
47 S. P. Wargacki, L. A. Lewis, M. D. Dadmun, *J. Forensic Sci.,* 2008, **53**, 1138.
48 C. Lennard, *Personal Commun.,* 2010.